# *Releasable Layer-by-Layer Assembly of Stabilized Lipid Nanocapsules on Microneedles for Enhanced Transcutaneous Vaccine Delivery*

Published in final edited form as:
*ACS Nano*. 2012 September 25; 6(9): 8041–8051. doi:10.1021/nn302639r.

# Releasable Layer-by-Layer Assembly of Stabilized Lipid Nanocapsules on Microneedles for Enhanced Transcutaneous Vaccine Delivery

**Peter C. DeMuth**[1,#], **James J. Moon**[1,2,#], **Heikyung Suh**[1,2,7], **Paula T. Hammond**[3,4,5], and **Darrell J. Irvine**[1,2,4,5,6,7]

[1]Department of Biological Engineering, Massachusetts Institute of Technology, 77 Massachusetts Ave, Cambridge, MA 02139

[2]Department of Materials Science and Engineering, Massachusetts Institute of Technology, 77 Massachusetts Ave, Cambridge, MA 02139

[3]Department of Chemical Engineering, Massachusetts Institute of Technology, 77 Massachusetts Ave, Cambridge, MA 02139

[4]Koch Institute for Integrative Cancer Research, Massachusetts Institute of Technology, 77 Massachusetts Ave, Cambridge, MA 02139

[5]Institute for Soldier Nanotechnologies, Massachusetts Institute of Technology, 77 Massachusetts Ave, Cambridge, MA 02139

[6]Ragon Institute of MIT, MGH, and Harvard, Boston, MA 02114, Institute for Soldier Nanotechnologies

[7]Howard Hughes Medical Institute 4000 Jones Bridge Rd., Chevy Chase, MD 20815

## Abstract

Here we introduce a new approach for transcutaneous drug delivery, using microneedles coated with stabilized lipid nanocapsules for delivery of a model vaccine formulation. Poly(lactide-*co*-glycolide) (PLGA) microneedle arrays were coated with multilayer films *via* layer-by-layer (LbL) assembly of a biodegradable cationic poly(β-amino ester) (PBAE) and negatively-charged interbilayer-crosslinked multilamellar lipid vesicles (ICMVs). To test the potential of these nanocapsule-coated microneedles for vaccine delivery, we loaded ICMVs with a protein antigen and the molecular adjuvant monophosphoryl lipid A (MPLA). Following application of microneedle arrays to the skin of mice for 5 minutes, (PBAE/ICMV) films were rapidly transferred from microneedle surfaces into the cutaneous tissue, and remained in the skin following removal of the microneedle arrays. Multilayer films implanted in the skin dispersed ICMV cargos in the treated tissue over the course of 24 hours *in vivo*, allowing for uptake of the lipid nanocapsules by antigen presenting cells (APCs) in the local tissue and triggering their activation *in situ*. Microneedle-mediated transcutaneous vaccination with ICMV-carrying multilayers promoted robust antigen-specific humoral immune responses with a balanced generation of multiple IgG isotypes, whereas bolus delivery of soluble or vesicle-loaded antigen *via* intradermal injection or transcutaneous vaccination with microneedles encapsulating soluble protein elicited weak, $IgG_1$-biased humoral immune responses. These results highlight the

*Corresponding authors: Prof. D. J. Irvine and Prof. P.T. Hammond. hammond@mit.edu, djirvine@mit.edu.
#These authors contributed equally to this work.

Supporting Information Available: Chemical structures of reagents, additional AFM and CLSM analysis, and characterization of multilayers containing soluble ovalbumin. This material is available free of charge *via* the Internet at http://pubs.acs.org.

potential of lipid nanocapsules delivered by microneedles as a promising platform for non-invasive vaccine delivery applications.

**Keywords**

layer-by-layer; transcutaneous delivery; microneedles; vaccine; polymer assembly; biodegradable

The generation of polyelectrolyte multilayers (PEMs) through the iterative and sequential adsorption of complimentary materials is an attractive approach for nanoscale assembly of functional systems capable of controlled encapsulation and delivery of diverse therapeutics. The inherent adaptability of multilayer processing, as well as its biocompatibility, scalability, and simplicity make it an ideal strategy for the creation of conformal coatings on complex surfaces (reviewed in [1, 2]). Recently, multilayers have been optimized for the encapsulation of lipid vesicles, with the aim of increasing the drug loading capacity of multilayer films, allowing for biological cargos to be entrapped in films in native aqueous conditions, and providing triggered materials release through programmed vesicle disruption.[3–10] A key issue for incorporation of liposomal carriers in multilayer films is the need for stabilization of vesicles against rupture during the assembly process or drying of the resulting films. Previous approaches have relied on vesicle stabilization strategies such as *in situ* silica polymerization[3, 4] or polyelectrolyte adsorption on the vesicle surface prior to multilayer assembly.[5–10] Without such stabilizing measures, LbL deposition results in spontaneous vesicle disruption into lipid bilayers on the target substrate.

We recently reported a new approach for lipid vesicle stabilization, where covalent crosslinks are introduced between adjacent phospholipid bilayers in the walls of multilamellar vesicles to create robust lipid nanocapsules.[11, 12] These interbilayer-crosslinked multilamellar vesicles (ICMVs) encapsulate protein cargos within their interior and exhibit enhanced serum stability in extracellular conditions, but can be readily degraded upon cellular internalization.[11] Vaccination with ICMVs elicited potent cellular and humoral immune responses against the model antigen ovalbumin (OVA), and enhanced long-term humoral responses to a recombinant malaria antigen following subcutaneous injection.[11, 12] Given their enhanced stability and unique potency in the context of protein vaccine delivery, we hypothesized that LbL deposition of ICMVs would provide an interesting opportunity for the design of ICMV-containing multilayer delivery systems for subunit vaccination.

In parallel studies, we and others have recently demonstrated the utility of microneedle arrays for the safe, rapid, and convenient delivery of drugs through the pain-free disruption of the stratum corneum to access the immune-competent epidermal and dermal tissue.[13–15] Microneedles have particularly shown promise in vaccine delivery.[15–17] Microneedle application is known to improve safety, eliminate pain upon treatment, and reduce the generation of hazardous medical waste associated with needle-based delivery.[18–20] Further, creation of conformal surface coatings on microneedle arrays has proven to be an effective method for therapeutic formulation and delivery into the skin *via* rapid, topical microneedle application.[15, 21] We therefore set out to design a PEM system for the stable encapsulation and release of ICMVs for transcutaneous delivery into the skin *via* microneedle insertion. We envisioned several potential advantages for such an approach including (i) improved dry state storage through PEM-embedding of ICMVs, (ii) controlled encapsulation and release of ICMVs from degradable PEMs implanted in the skin, (iii) delivery of ICMVs to an inherently immunogenic tissue for enhanced immunity through microneedle application, and (iv) convenient and self-contained combination of vaccine and administration device for rapid, safe, and painless vaccine delivery that could potentially be self-administered in minutes.

Here we report studies intended to test these hypotheses, focusing on the generation of a PEM system capable of stable ICMV encapsulation and release for protein immunization. We first show the ability of degradable PEMs to stably incorporate ICMV particles, both on flat silicon substrates as well as PLGA microneedles, controlling film thickness and ICMV dosage, and verifying that incorporated ICMVs are intact within dried multilayer films. We then demonstrate the ability for PEM-coated microneedles to transfer their ICMV-loaded films into the cutaneous tissue upon brief application to the skin of mice. Following film degradation and ICMV dispersion in the epidermal tissue, ICMVs were found to be taken up by resident APCs within the skin, which were activated *in situ* by adjuvants delivered by the particles. Finally, we show that transcutaneous vaccination with ICMVs embedded in microneedle-based multilayers significantly enhanced humoral immune responses to a protein antigen, compared to mice vaccinated with either conventional intradermal bolus injection of antigen or microneedle-mediated delivery of soluble protein antigen. Together, these results suggest the potential of microneedle-based multilayers for the effective transcutaneous delivery of functional nanoscale vesicles. In this work, we have improved protein subunit vaccination by taking advantage of the immunogenicity of ICMVs delivered to the skin, a site known for high frequency of epidermal and dermal APCs; however, this work describing vesicle deposition on multilayer-coated microneedles can be readily adapted as a modular, general strategy for non-invasive drug delivery to the skin.

## RESULTS AND DISCUSSION

We recently demonstrated that microneedles coated with PLGA nanoparticle-loaded PEMs could be used for rapid implantation of particle-loaded films in skin.[15] PLGA particles are attractive for small-molecule drug delivery but have limitations for delivery of biologics such as vaccines, due to the low doses of proteins that can be encapsulated and the potential for antigen denaturation during processing. We hypothesized that the deposition of an ICMV-containing multilayer coating on the surface of microneedles would provide a solution to these issues and enable a simple, self-contained, and effective method for recombinant protein vaccine storage and delivery to the skin, an attractive tissue target due to its dense matrix of resident innate immune cells (Figure 1).[22–24] To fabricate an erodible PEM system capable of encapsulating and delivering intact nanoscale vesicles we selected Poly-1 (Figure S1) a biocompatible, hydrolytically degradable polymer from a class of polyelectrolytes known as poly($\beta$-amino esters) (PBAEs), to serve as a complimentary degradable partner for ICMV encapsulation in multilayers. Poly-1 has been extensively studied in a variety of contexts and has been proven effective in generating erodible multilayer films containing many diverse cargos for controlled drug release.[15, 21, 25–29] We selected ICMVs to serve as a stable poly-anionic vesicular partner for Poly-1 in multilayer deposition, taking advantage of their colloidal stability and potency as vaccine delivery vehicles.[11, 12] In this context, ICMVs could serve as a modular delivery vehicle for antigen and adjuvant incorporated either in the aqueous vesicle core or the hydrophobic lipid capsule walls of ICMVs, and the covalent inter-bilayer maleimide crosslinks would provide stability for multilayer encapsulation (Figure 1a). We hypothesized that (Poly-1/ICMV) multilayers would be deposited into the skin through brief topical microneedle application (Figure 1b), where hydrolytic degradation of Poly-1 over time would lead to ICMV release (Figure 1c) into the surrounding tissue, followed by uptake into local APCs (Figure 1d) that would initiate adaptive immunity.

Negatively-charged ICMVs encapsulating fluorescent OVA and composed of DOPC and maleimide-lipid MPB (Figure S1) in a 1:1 mole ratio (diam. 240 ± 10 nm, 0.19 ± 0.05 polydispersity index, zeta potential −41 ± 1.0 mV, incorporating 0.1 wt% DiI as a fluorescent tracer in the vesicle walls) were prepared as previously described.[11, 12] To determine whether ICMVs could be stably embedded into degradable multilayer films, we

first synthesized model LbL films on atomically-flat silicon substrates. First, 20 bilayers of protamine sulfate (PS) and sulfonated poly(styrene) (SPS) were deposited to form a base layer of uniform surface charge.[15, 30] Through subsequent LbL steps, we attempted to construct ICMV-encapsulating multilayers through sequential immersion in aqueous Poly-1 and ICMV suspensions of varying concentrations. As shown in Figure 2a, when LbL assembly was performed using ICMVs at 0.5 mg/ml in phosphate buffered saline (PBS) at pH 5.0, we observed insignificant and irregular film growth, with film thickness remaining steady after 15 deposition cycles at ~400 nm as measured by profilometry. However, using a more concentrated 1 mg/ml ICMV dispersion, we observed a regular linear increase in measured film thickness (~50 nm/bilayer) with each deposition cycle up to 35 rounds of LbL deposition, resulting in films more than 1.5 μm thick (Figure 2a). For comparison with the crosslink-stabilized ICMVs, we also synthesized non-crosslinked multilamellar vesicles (MLVs) *via* the same process used to prepare ICMVs, leaving out the final interbilayer crosslinking step. In contrast to ICMVs, MLVs (diam. 270 ± 17 nm, 0.23 ± 0.014 polydispersity index, zeta potential −33.6 ± 0.9 mV) displayed inconsistent and irregular film growth plateauing at ~500 nm after 15 bilayers (Figure 2a). This result is consistent with previous evidence showing ineffective LbL growth of phospholipid vesicles without sufficient stabilization to prevent spontaneous disruption upon adsorption.[31, 32] Spectroscopic measurement of fluorescent signal obtained after (Poly-1/ICMV) film disruption in NaCl for 24 hours indicated a loading of ~5 μg OVA/cm$^2$ and ~15 μg lipids/cm$^2$ for multilayers containing 35 bilayers (~1.6 μm in thickness), consistent with the known OVA loading density of intact ICMVs;[11] this loading is within the effective dose range needed for ICMVs to generate potent immune responses *in vivo* when administered by traditional routes.[11, 12] Further, previous studies have demonstrated enhanced potency of transcutaneously-administered vaccines, suggesting that additional dose sparing might be possible in this context.[33–35]

Given the success of film growth at these initial conditions, we then measured the effect of deposition time on the growth of (Poly-1/ICMV) containing films, and observed no significant increase in film growth per bilayer when the duration for Poly-1 and ICMV adsorption was increased from 5 to 10 minutes (Figure 2b). We thus concluded that 5 minutes was a sufficient time period to achieve ICMV adsorption and reversal of surface charge for successful LbL adsorption. To confirm that ICMVs were stably incorporated into Poly-1 films, we performed confocal laser scanning microscopy (CLSM) on (Poly-1/ICMV) multilayers constructed using ICMVs labeled with DiI in the lipid phase of the particles and encapsulating fluorescent AF647-OVA. CLSM imaging showed the presence of overlaid punctate fluorescent signals indicating colocalization of AF647-OVA and DiI in submicron spherical particles, suggesting the incorporation of intact, OVA-loaded ICMVs into Poly-1 multilayers (Figure 2c). This punctate fluorescent signal was not observed in films constructed using MLVs formed in the absence of interbilayer crosslinks, and only low levels of OVA fluorescence were detected in such films, providing evidence for the importance of the stabilizing inter-bilayer crosslinks of ICMVs for preventing vesicle disruption during LbL processing (Figure 2c). In addition, large contiguous patches of the DiI lipid tracer were observed in films prepared with non-crosslinked MLVs, suggesting fusion among vesicles occurring in this case (Figure 2c). To obtain further confirmation of intact ICMV incorporation into multilayers, we performed atomic force microscopy (AFM) to investigate the surface of (Poly-1/ICMV) films on silicon. Consistent with previous studies showing intact vesicle incorporation,[3, 4, 8–10] we observed individual spherical structures 100–300 nm in diameter in height and phase AFM images, suggesting that multilayer-embedded ICMVs were intact and unchanged following LbL deposition (Figure 2d–e). This was readily apparent upon 3-D rendering of AFM height data (Figure 2f) and in analysis of height traces (Figure 2g), suggesting individual ICMVs embedded within the (Poly-1/ICMV) multilayers. The exposed dimensions of particles at the top of films

measured in this way showed diameters of ~100–300 nm and heights of ~50–75 nm, consistent with the previously measured average bilayer thickness and suggesting some deformation and burial of the particles in underlying Poly-1 layers, as observed in prior studies of vesicles incorporated in multilayers.[6, 9] Additional AFM measurement of dry films stored at room temperature for 7 days revealed similar punctate patterns with no significant change in dimension, indicating the potential for multilayer encapsulated ICMVs to maintain their structure upon dry-state storage (Figure S2), an attractive feature for potential vaccine delivery systems in the developing world.

Given the ability of Poly-1 multilayers to encapsulate intact ICMVs, we next sought to use this approach for ICMV delivery and release into the skin. We and others have recently reported the successful generation of multilayer films on the surface of microneedle arrays for transcutaneous delivery *in vivo*.[15, 21] We hypothesized that a similar approach could allow for ICMV-loaded multilayer delivery, and given the demonstrated potency of ICMVs for generating adaptive immunity,[11, 12] we anticipated that ICMV delivery to the APC-rich epidermis might provide enhanced dose sparing immunogenicity. To test whether ICMV-loaded multilayers could be deposited as surface coatings on microneedles, we first fabricated PLGA microneedles using poly(dimethyl siloxane) (PDMS) molding as previously described,[15] yielding arrays of conical microneedles each ~650 μm in height and 250 μm in diameter at the base. Then, following (PS/SPS) base-layer deposition on these microneedles, we performed LbL assembly using fluorescently-labeled DiI-ICMVs encapsulating AF647-OVA as before. CLSM on the resulting multilayer-coated microneedles revealed consistent and uniform fluorescent signal localized to the surface of each microneedle, indicating effective multilayer deposition as observed for flat silicon substrates (Figure 3a). Using confocal z-scanning, we then performed quantitative analysis of the total fluorescent signal on individual microneedles following deposition of 10, 20, or 30 bilayers. This analysis demonstrated a similar linear growth profile for both DiI-labeled ICMVs and the encapsulated AF647-OVA cargo, consistent with the thickness increase measured with profilometry on silicon (Figure 3b). In addition to confirming the similar growth of silicon- and microneedle-based films, these results provide additional evidence for intact ICMV incorporation on microneedle surfaces, consistent with our previous demonstration of nanoparticle encapsulation on microneedle arrays through spray LbL deposition.[15] Finally, we imaged the resulting multilayer-coated microneedles using scanning electron microscopy (SEM) and observed the presence of consistent surface coatings uniformly covering the entire microneedle array surface (Figure 3c).

We next tested whether microneedle-based multilayers encapsulating ICMVs were delivered into skin following microneedle application *in vivo*. We have previously shown that microneedles similar to those used here are effective in providing consistent disruption of the stratum corneum and insertion into the outer layers of the skin following brief topical application to the skin of mice.[15] We confirmed this result using trypan blue staining of treated skin and observed uniform staining patterns indicating microneedle insertion as before (data not shown). To test for transcutaneous delivery, multilayer-coated microneedles carrying AF647-OVA-loaded, DiI-labeled ICMVs were applied to the dorsal ear or flank skin of C57Bl/6 mice. We then performed quantitative CLSM image analysis to determine the relative loss of fluorescent signal from individual microneedles following application. Microneedles applied for only 5 minutes showed significant losses of both DiI and AF647-OVA fluorescent signal over the entire microneedle surface, with ~80% reduction in fluorescent intensity observed on the microneedle surfaces (Figure 4a–c). Fluorescent signal reduction was equivalent for both the lipophilic tracer and protein cargo, suggesting delivery of intact multilayer-embedded ICMVs. These results are consistent with our previous demonstration of polymer nanoparticle-loaded multilayer delivery, in which we observed that, unlike multilayers composed only of polymeric materials, PEMs containing embedded

particles were rapidly transferred to the skin after brief application of microneedle arrays.[15] This difference in the kinetics of multilayer transfer may reflect a decreased degree of interpenetrating molecular entanglements between complementary polymer and nanoparticle pairs, compared to multilayers composed of complementary polymers alone. The microneedles themselves make up 45% of the total coated surface area on the microneedle array, meaning that with 80% delivery of the coated material, overall ~36% of the vaccine components coated on the microneedles are estimated to be delivered into the skin. Approaches to increase this fraction can be readily envisioned by using a hydrophobic base to prevent wetting of the backing and/or employing strategies to carry out LbL deposition only on the microneedle tips.[21, 36]

We next examined microneedle-treated skin to observe deposition of ICMV-loaded multilayers into the tissue. ICMVs were prepared with AF647-OVA loaded in the aqueous core as a model protein antigen. As adjuvants to provide local inflammatory cues necessary to drive the immune response, we embedded the Toll like receptor (TLR)-4 agonist MPLA in the ICMV capsule walls, and further applied aqueous solutions of the TLR-3 agonist polyI:C (a double-stranded RNA mimic of viral RNA) directly to the skin just prior to microneedle application. To observe ICMV delivery in relation to target APC populations in the skin, we applied microneedles to the skin of MHC II-GFP mice. These animals express all major histocompatibility class II (MHC II) molecules as a fusion with green fluorescent protein (GFP), allowing MHC $II^+$ APCs in the viable epidermis/dermis to be observed through CLSM imaging in auricular or flank skin.[37] Microneedles were applied to ear skin for 5 min, which was then dissected 6 or 24 hr later for CLSM imaging. After 6 hr, we observed AF647-OVA and DiI fluorescence in clusters around microneedle insertion sites; these signals were colocalized in the same *z*-plane as epidermal APCs expressing MHC II-GFP and extended several hundred microns below the skin surface (Figure 4d and S3). In skin collected 24 hours following treatment, we observed similar fluorescent signal colocalization (Figure 4e) at microneedle insertion sites. However, after 24 hours, low and high magnification CLSM imaging revealed the emergence of punctate fluorescent signal dispersed throughout the tissue, similar to that observed for multilayer-embedded ICMVs, suggesting multilayer disintegration and release/diffusion of ICMVs *in situ* (Figure 4e–f). This finding is consistent with the known degradation kinetics of Poly-1 multilayers, which undergo complete breakdown within 24 hours.[15, 38] Dispersed particles were consistently localized within the viable epidermal layers as evidenced by colocalization within the same z-plane as MHC II-$GFP^+$ APCs (likely Langerhans cells). Further imaging indicated direct interaction between epidermal APCs and ICMVs within the treated skin, as $GFP^+$ cells were observed with internal fluorescent signal from both AF647-OVA and DiI (Figure 4f). In some cases, MHC II-$GFP^+$ APCs were observed with membrane extensions around punctate fluorescent particles, suggesting that ICMVs released from implanted multilayers were actively being phagocytosed by resident immune cells in the skin (Figure 4g).

The presence of TLR-3 and TLR-4 molecular adjuvants triggered striking changes in the APC populations present in the skin of mice with implanted ICMV multilayers (Figure 5). To determine the effect of co-delivery of ICMVs with MPLA and polyI:C, mice were treated with either uncoated microneedles, or microneedle arrays delivering ICMVs with or without MPLA and polyI:C. A representative series of CLSM images from the 6 and 24 hour timepoints following treatment were analyzed using Image J software particle analysis algorithms[39] to determine various phenotypically significant parameters including total cell number per field, individual cell area and perimeter, and individual cell MHC II-GFP mean fluorescent intensity (MFI). From representative CLSM fields (Figure 5a–b), as well as the dependent quantitative analysis, we observed a dramatic increase in MHC $II^+$ cells present in the skin tissue between 6 and 24 hours for mice treated with polyI:C and microneedles coated with ICMVs encapsulating OVA with MPLA, compared to microneedles alone or

microneedles coated with only ICMVs (Figure 5c). This recruitment of APCs to the microneedle application site contrasts with recent studies using microneedle arrays composed of shorter (100 μm in length) silicon needles (either bare or coated with antigens and saponin adjuvants), where a slight decrease in the density of MHC $II^+$ cells was observed by 24 hr, suggesting activation and migration of dendritic cells toward lymphatics following patch application.[40, 41] However, APC accumulation is consistent with the normal physiological response to inflammation following vaccination, as local chemokine release from stimulated keratinocytes and innate immune cells triggers both resident cell division and homing of blood-borne APCs to the inflamed tissue microenvironment.[22–24] Notably, prior studies using adjuvants such as the TLR agonist imiquimod[42] or cytokines such as GM-CSF or FLT-3L[43, 44] have shown similar infiltration of dendritic cells to skin vaccination sites (including in human trials), which correlates with greater frequencies of antigen-carrying APCs arriving at draining lymph nodes. Such dramatic APC recruitment to the application site was not observed for bare microneedles, suggesting that the response observed in this study vs. the silicon microneedle studies cited above are not simply due to greater wounding of the skin by the larger microneedles used here.

In addition, TLR agonists trigger activation of APCs, which is accompanied by morphological changes and upregulation of MHC expression,[45–47] which we also saw reflected in skin treated with ICMVs with MPLA and polyI:C. Here individual $GFP^+$ APCs were observed to take on an extended dendritic morphology (Figure 5a, b) and increase in area (~3x), perimeter (~2x), and mean MHC II-GFP fluorescence intensity (~10x, Figure 5c) as compared to bare microneedle or ICMV-only treatments. Together these parameters are indicative of a shift towards an activated phenotype in APCs, as stimulated dendritic cells increase cellular processes to more effectively capture antigen and increase expression of MHC II for effective communication with naive lymphocytes in the generation of adaptive immunity. Thus, we have observed the effective delivery of ICMV-containing multilayers from microneedle arrays into treated skin, the subsequent disintegration of multilayer depots releasing ICMVs, which are dispersed throughout the skin for uptake by resident APCs, ultimately resulting in coincident antigen delivery and activation and maturation of the resident APC population.

Finally, we tested whether transcutaneous administration of microneedle-based multilayers encapsulating ICMVs could elicit immune responses against an antigen incorporated within ICMVs. Groups of C57Bl/6 mice were immunized on day zero and given booster immunizations after 4 weeks and 8 weeks with 1 μg OVA (model antigen), 0.03 μg MPLA, and 10 μg polyI:C. For each immunization, mice received transcutaneous administration of microneedles delivering Poly-1 multilayers encapsulating either ICMVs (containing OVA and MPLA, OVA-ICMV-MN) or equivalent doses of soluble OVA (OVA-MN, Figure 6a). In both cases microneedle multilayer delivery was performed in the presence of soluble polyI:C (and MPLA in the case of OVA multilayers) applied to the skin surface before treatment. Multilayers loaded with soluble OVA were constructed based upon previously reported methods adapted for microneedle deposition.[27] Characterization of OVA-multilayer loading and delivery *in vivo* demonstrated effective OVA loading into microneedle-based multilayers, and efficient transcutaneous delivery upon microneedle application (Figure S4). To further delineate the efficacy of microneedle-based transcutaneous vaccination from conventional bolus injection of immunogens, we also vaccinated control groups of mice by intradermal injection of ICMVs (containing OVA and MPLA, OVA-ICMV-ID) with polyI:C or soluble formulations delivering the same doses of antigen and adjuvants as in the microneedle treated groups (OVA-ID, Figure 6a). All groups received the same total dose of OVA, MPLA, and polyI:C. Notably, following the first booster immunization all groups responded with increased OVA-specific serum IgG titers, and the total IgG titer of ICMV vaccines were identical for injected vs. microneedle

formulations by day 56 (Figure 6b). However, only mice immunized with microneedle delivery of ICMV-carrying multilayers responded to the second boost at day 56, with serum IgG titers showing an additional >10-fold increase for this group, while the other immunization regimens elicited stable or declining titers at subsequent timepoints. The need for multiple vaccinations to achieve this high titer is offset by the potential for enhanced protection by such a substantial increase in strength of the humoral response and the self-administrable nature of microneedle patch vaccines. We further analyzed sera obtained on day ~110 post-immunization to determine the isotypes of antibodies generated by transcutaneous vs. intradermal administration of either soluble or ICMV vaccine formulations. Vaccination with free OVA protein either *via* microneedles or intradermal injection resulted in Th2-biased $IgG_1$ responses without any detectable level of Th1-associated $IgG_{2c}$ antibodies (Figure 6c, d). In contrast, ICMVs administered by traditional syringe intradermally or delivered by multilayer-coated microneedles elicited a more balanced Th1/Th2 response with both $IgG_1$ and $IgG_{2c}$ titers, with transcutaneous delivery of ICMV-carrying microneedles achieving 10-fold higher $IgG_{2c}$ titers than “free” ICMV injection (Figure 6c, d). This is of interest since $IgG_2$ antibody isotypes have been implicated in enhanced protection in both infectious disease and cancer vaccines.[48–50] Thus, these results suggest that microneedle-based multilayers encapsulating ICMVs are a promising platform for delivery of vaccine antigen and adjuvant to skin-resident APCs *via* a non-invasive, needle-free route for promotion of long-lived, high-titer humoral immune responses.

## CONCLUSIONS

In summary, we have shown the successful incorporation of intact multilamellar phospholipid vesicles into erodible multilayer films through the use of an inter-bilayer molecular crosslinking stabilization strategy. We have further demonstrated the potential utility of such functional multilayer coatings constructed on microneedle arrays for rapid transfer of particle-carrying multilayers into microneedle-treated skin, and for the subsequent release of vesicle cargos through multilayer degradation *in situ*. Thus, this platform may ultimately serve as a potent platform for protein vaccination providing enhanced immunogenicity, simple and safe administration, and the potential for dry-state storage. These advantages provide the opportunity for more effective and less costly vaccine storage and distribution to the developing world, as multilayer stabilized formulations could be stored easily without refrigeration until rehydration upon microneedle insertion into the target tissue. Though we employed a LbL dipping process in multilayer fabrication for these lab-scale studies for convenience, note that commercial scale processes could readily employ spray deposition to eliminate loss of precious vaccine materials during fabrication.[51] The combination of multilayer deposition with microneedle application for transcutaneous delivery also addresses the need for a safe, potent, and non-invasive alternative to hypodermic needle-based administration. The simplicity of microneedle application also provides the prospect of rapid self-administration potentially streamlining mass vaccination and eliminating the need for healthcare worker training.[34, 52, 53] In addition, the ability of ICMVs and multilayers to incorporate diverse drug compounds and biologics makes this approach of broader interest for enhanced transcutaneous delivery of therapeutics.

## METHODS

### Materials

Poly-1 (16 kDa) was synthesized according to previous literature.[26] Alexa Fluor 647-conjugated ovalbumin, and 1,1′-dilinoleyl-3,3,3′,3′-tetramethylindocarbocyanine (DiI) were purchased from Invitrogen (Eugene, OR). PLGA (50:50, IV 1.9 dL/g) was purchased from Lakeshore Biomaterials (Birmingham, AL). DOPC (1,2-Dioleoyl-*sn*-Glycero-3-

Phosphocholine) and MPB (1,2-dioleoyl-*sn*-glycero-3-phosphoethanolamine-N-[4-(p-maleimidophenyl) butyramide) were purchased from Avanti Polar Lipids (Alabaster, AL). MPLA was purchased from Sigma Aldrich (St. Louis, MO). PolyI:C was obtained from Invivogen (SanDiego, CA). Chromatographically purified ovalbumin, purchased from Worthington (Lakewood, NJ), was processed through Detoxi-Gels (Pierce, Rockford, IL) to remove any residual endotoxin.

### PLGA Microneedle Fabrication

PDMS molds (Sylgard 184, Dow Corning) were fabricated by laser ablation using a Clark-MXR CPA-2010 micromachining system (VaxDesign Inc.). PLGA pellets (IV 0.35 dL/g) were melted over the molds under vacuum (−25 in. Hg) at 140°C for 40 min, and then cooled to −20°C before separating the cast PLGA microneedles from the PDMS mold. Microneedles were characterized by SEM using a JEOL 6700F FEG-SEM.

### ICMV Synthesis

Synthesis of ICMVs was performed as described previously.[11, 12] Briefly, dried films of 1.26 μmol of lipids (DOPC:MPB at 1:1 mol ratio) and 2.9 μg of MPLA were rehydrated in 20 mM bis-tris propane at pH 7.0 with 325 μg ovalbumin for 1 hr with vortexing every 10 min, and sonicated in alternating power cycles of 6 watts and 3 watts in 30s intervals for 5 min on ice (Misonix Microson XL probe tip sonicator, Farmingdale, NY). DTT and $Ca^{2+}$ were then sequentially added at final concentrations of 3 mM and 40 mM, respectively, and incubated for 1 hr at 37°C to form ICMVs. The particles were recovered by centrifugation, washed twice, resuspended in PBS at pH 5.0, and stored at 4°C until usage. In some experiments, ICMVs were prepared including a lipophilic tracer, DiI, at 0.2 molar % concentration, and 325 μg of Alexa Fluor 647-conjugated OVA was used to hydrate the lipid films.

### Multilayer Film Preparation

All LbL films were assembled using a Carl Ziess HMS DS50 slide stainer. Films were constructed on Si wafers and PLGA microneedle arrays. To build (PS/SPS) base layers, substrates were dipped alternatively into PS (2 mg/mL, PBS, Sigma-Aldrich) and SPS (5 mM, PBS, Sigma-Aldrich) solutions for 10 min, separated by two sequential 1 min rinses in PBS. (Poly-1/ICMV) and (Poly-1/MLV) multilayers were deposited similarly, alternating 5 min dips in Poly-1 (2 mg/mL, PBS) and ICMV/MLV solutions (1 mg/mL, PBS) separated by two sequential 30 sec rinsing steps in PBS. (Poly-1/OVA) multilayers were deposited by alternating 10 min dips in Poly-1 (2 mg/mL, 0.2M sodium acetate) and OVA solutions (0.1 mg/mL, 0.2M sodium acetate) separated by two sequential 1 min rinsing steps in deionized water. All solutions were adjusted to pH 5.0 and filtered (0.2μm, except ICMV/MLV and OVA) prior to dipping.

### Multilayer Film Characterization

Film thickness on Si wafers was characterized using a Veeco Dektak (Plainview, NY) surface profilometer and a Veeco Dimension 3100 AFM. Film growth and morphology on PLGA microneedles was characterized by SEM using a JEOL 6700F FEG-SEM and CLSM using a Carl Zeiss LSM 510. Data analysis was performed using Image J[39] and Graphpad Prism (La Jolla, CA). Film loading was determined for fluorescent cargos using a SpectraMax 250 spectrophotometer (Molecular Devices, Sunnyvale, CA) following elution of films in PBS, pH 7.4, 2M NaCl for 24 hours.

### Characterization of Film Delivery *In Vivo*

ICMV or soluble OVA delivery was measured *in vivo* following application of coated microneedles to the skin of mice. Animals were cared for in the USDA-inspected MIT Animal Facility under federal, state, local, and NIH guidelines for animal care. Microneedle application experiments were performed on anesthetized 6–10-week-old female C57BL/6 (Jackson Laboratories) and C57Bl/6-MHC II-GFP transgenic mice (a gift from Prof. Hidde Ploegh, MIT) at the dorsal ear or flank skin. Skin was rinsed briefly with PBS and dried before application of microneedle arrays by gentle pressure. Following application, mice were euthanized at subsequent time points and the application site was dissected. Excised skin was stained with trypan blue before imaging for needle penetration. In separate experiments treated skin and applied microneedle arrays were imaged by confocal microscopy to assess transcutaneous delivery of encapsulated ICMVs or soluble OVA. MHC II-GFP$^+$ cell number and morphology were analyzed by CLSM in dissected tissue following microneedle treatment. Image analysis was performed using NIH Image J software.[39]

### Vaccinations and Characterization of Humoral Immune Responses

Groups of 6–10-wk old female C57Bl/6 mice were immunized on days 0, 28, and 56 with 1 μg OVA, 0.03 μg MPLA, and 10 μg polyI:C either in suspension or microneedle formulations. Microneedle coating compositions were chosen so that the dose of antigen/MPLA delivered into the skin matched the injected cases: microneedle coatings were dissolved in sodium chloride buffer and the amount of antigen present was assessed using a spectrofluorimeter for as-prepared and post-skin-application microneedles; the delivered dose was determined as the difference between these two values. For intradermal administration, immunogens in 15 μL PBS were injected intradermally in the dorsal auricular skin. Transcutaneous administration of microneedles was performed as described above, following brief rinsing with sterile PBS at the dorsal ear skin. For multilayers containing OVA/MPLA-loaded ICMVs, polyI:C was administered in 5μl PBS to the surface of the skin prior to treatment and left in place during the duration of microneedle application. For multilayers containing soluble OVA, polyI:C and MPLA were similarly administered to the skin prior to microneedle treatment. Microneedles were secured in place for 5 minutes for both ICMV- and soluble OVA-containing multilayer coating variations. Sera obtained from immunized mice at various time points were analyzed for IgG, $IgG_1$, and $IgG_{2c}$ antibodies by ELISA using OVA-coated plates Anti-OVA IgG titers were defined as the lowest serum dilution at which the ELISA OD reading was ≥ 0.5.

### Statistical analysis

Data sets were analyzed using one- or two-way analysis of variance (ANOVA), followed by Tukey's HSD test for multiple comparisons with Prism 5.0 (GraphPad Software, San Diego, CA). *p*-values less than 0.05 were considered statistically significant. All values are reported as mean ± s.e.m.

## Supplementary Material

Refer to Web version on PubMed Central for supplementary material.

## Acknowledgments

This work was supported in part by the Ragon Institute of MGH, MIT, and Harvard, the NIH (AI095109), the MIT Institute for Soldier Nanotechnology, Army Research Office, and the Dept. of Defense (W911NF-07-D-0004 and W911NF-07-D-0004, T.O. 8). DJI is an investigator of the Howard Hughes Medical Institute.

## REFERENCES AND NOTES


1. DeVilliers MM, Otto DP, Strydom SJ, Lvov YM. Introduction to Nanocoatings Produced by Layer-by-Layer (LbL) Self-Assembly. Adv Drug Delivery Rev. 2011; 63:701–715.
2. Hammond PT. Engineering Materials Layer-by-Layer: Challenges and Apportunities in Multilayer Assembly. AIChE J. 2011; 57:2928–2940.
3. Katagiri K, Hamasaki R, Ariga K, Kikuchi J-i. Layered Paving of Vesicular Nanoparticles Formed with Cerasome as a Bioinspired Organic-Inorganic Hybrid. J Am Chem Soc. 2002; 124:7892–7893. [PubMed: 12095320]
4. Katagiri K, Hamasaki R, Ariga K, Kikuchi J-i. Layer-by-Layer Self-Assembling of Liposomal Nanohybrid “Cerasome” on Substrates. Langmuir. 2002; 18:6709–6711.
5. Graf N, Tanno A, Dochter A, Rothfuchs N, Voeroes J, Zambelli T. Electrochemically Driven delivery to Cells from Vesicles Embedded in Polyelectrolyte Multilayers. Soft Matter. 2012; 8:3641–3648.
6. Michel M, Arntz Y, Fleith G, Toquant J, Haikel Y, Voegel JC, Schaaf P, Ball V. Layer-by-Layer Self-Assembled Polyelectrolyte Multilayers with Embedded Liposomes: Immobilized Submicronic Reactors for Mineralization. Langmuir. 2006; 22:2358–2364. [PubMed: 16489829]
7. Michel M, Izquierdo A, Decher G, Voegel JC, Schaaf P, Ball V. Layer by Layer Self-Assembled Polyelectrolyte Multilayers with Embedded Phospholipid Vesicles Obtained by Spraying: Integrity of the Vesicles. Langmuir. 2005; 21:7854–7859. [PubMed: 16089392]
8. Michel M, Vautier D, Voegel JC, Schaaf P, Ball V. Layer by Layer Self-Assembled Polyelectrolyte Multilayers with Embedded Phospholipid Vesicles. Langmuir. 2004; 20:4835–4839. [PubMed: 15984239]
9. Volodkin D, Arntz Y, Schaaf P, Moehwald H, Voegel JC, Ball V. Composite Multilayered Biocompatible Polyelectrolyte Films with Intact Liposomes: Stability and Temperature Triggered Dye Release. Soft Matter. 2008; 4:122–130.
10. Volodkin DV, Schaaf P, Mohwald H, Voegel JC, Ball V. Effective Embedding of Liposomes into Polyelectrolyte Multilayered Films: the Relative Importance of Lipid-Polyelectrolyte and Interpolyelectrolyte Interactions. Soft Matter. 2009; 5:1394–1405.
11. Moon JJ, Suh H, Bershteyn A, Stephan MT, Liu H, Huang B, Sohail M, Luo S, Um SH, Khant H, et al. Interbilayer-Crosslinked Multilamellar Vesicles as Synthetic Vaccines for Potent Humoral and Cellular Immune Responses. Nat Mater. 2011; 10:243–251. [PubMed: 21336265]
12. Moon JJ, Suh H, Li AV, Ockenhouse CF, Yadava A, Irvine DJ. Enhancing Humoral Responses to a Malaria Antigen with Nanoparticle Vaccines that Expand Tfh Cells and Promote Germinal Center Induction. Proc Natl Acad Sci U S A. 2012; 109:1080–1085. [PubMed: 22247289]
13. Wermeling DP, Banks SL, Hudson DA, Gill HS, Gupta J, Prausnitz MR, Stichcomb AL. Microneedles Permit Transdermal Delivery of a Skin-Impermeant Medication to Humans. Proc Natl Acad Sci U S A. 2008; 105:2058–2063. [PubMed: 18250310]
14. Zhu Q, Zarnitsyn VG, Ye L, Wen Z, Gao Y, Pan L, Skountzou I, Gill HS, Prausnitz MR, Yang C, et al. Immunization by Vaccine-Coated Microneedle Arrays Protects Against Lethal Influenza Virus Challenge. Proc Natl Acad Sci U S A. 2009; 106:7968–7973. [PubMed: 19416832]
15. DeMuth PC, Su X, Samuel RE, Hammond PT, Irvine DJ. Nano-layered Microneedles for Transcutaneous Delivery of Polymer Nanoparticles and Plasmid DNA. Advanced Materials. 2010; 22:4851–4856. [PubMed: 20859938]
16. Chen X, Kask AS, Crichton ML, McNeilly C, Yukiko S, Dong L, Marshak JO, Jarrahian C, Fernando GJP, Chen D, et al. Improved DNA Vaccination by Skin-Targeted Delivery Using Dry-Coated Densely-Packed Microprojection Arrays. J Controlled Release. 2010; 148:327–333.
17. Sullivan SP, Koutsonanos DG, Del Pilar MM, Lee Jeong W, Zarnitsyn V, Choi Seong O, Murthy N, Compans RW, Skountzou I, Prausnitz MR. Dissolving Polymer Microneedle Patches for Influenza Vaccination. Nat Med. 2009; 16:915–20. [PubMed: 20639891]
18. Donatus U, Bruce G, Robert T. Model-Based Estimates of Risks of Disease Transmission and Economic Costs of Seven Injection Devices in Sub-Saharan Africa. Bull World Health Organ. 2002; 80:859–70. [PubMed: 12481207]

19. Pruss-Ustun, A.; Rapita, E.; Hutin, Y. Sharps injuries: global burden of disease from sharps injuries to health-care workers. World Health Organization; 2003.
20. Giudice EL, Campbell JD. Needle-Free Vaccine Delivery. Adv Drug Delivery Rev. 2006; 58:68–89.
21. Saurer EM, Flessner RM, Sullivan SP, Prausnitz MR, Lynn DM. Layer-by-Layer Assembly of DNA- and Protein-Containing Films on Microneedles for Drug Delivery to the Skin. Biomacromolecules. 2010; 11:3136–3143.
22. Kupper TS, Fuhlbrigge RC. Immune Surveillance in the Skin: Mechanisms and Clinical Consequences. Nat Rev Immunol. 2004; 4:211–222. [PubMed: 15039758]
23. Merad M, Ginhoux F, Collin M. Origin, Homeostasis and Function of Langerhans Cells and Other Langerin-Expressing Dendritic Cells. Nat Rev Immunol. 2008; 8:935–947. [PubMed: 19029989]
24. Nestle FO, Di Meglio P, Qin JZ, Nickoloff BJ. Skin Immune Sentinels in Health and Disease. Nat Rev Immunol. 2009; 9:679–691. [PubMed: 19763149]
25. Jewell CM, Lynn DM. Multilayered Polyelectrolyte Assemblies as Platforms for the Delivery of DNA and Other Nucleic Acid-Based Therapeutics. Adv Drug Delivery Rev. 2008; 60:979–999.
26. Lynn DM, Langer R. Degradable Poly(Beta-amino esters): Synthesis, Characterization, and Self-Assembly with Plasmid DNA. J Am Chem Soc. 2000; 122:10761–10768.
27. Su X, Kim BS, Kim Sara R, Hammond Paula T, Irvine Darrell J. Layer-by-Layer-Assembled Multilayer Films for Transcutaneous Drug and Vaccine Delivery. ACS Nano. 2009; 3:3719–29. [PubMed: 19824655]
28. Akinc A, Anderson DG, Lynn DM, Langer R. Synthesis of Poly(Beta-Amino Ester)s Optimized for Highly Effective Gene Delivery. Bioconjugate Chem. 2003; 14:979–988.
29. Greenland JR, Liu H, Berry D, Anderson DG, Kim WK, Irvine DJ, Langer R, Letvin NL. Beta-Amino Ester Polymers Facilitate in Vivo DNA Transfection and Adjuvant Plasmid DNA Immunization. Mol Ther. 2005; 12:164–170. [PubMed: 15963932]
30. Samuel RE, Shukla A, Paik DH, Wang MX, Fang JC, Schmidt DJ, Hammond PT. Osteoconductive Protamine-Based Polyelectrolyte Multilayer Functionalized Surfaces. Biomaterials. 2011; 32:7491–7502. [PubMed: 21764442]
31. Ichinose I, Fujiyoshi K, Mizuki S, Lvov Y, Kunitake T. Layer-by-Layer Assembly of Aqueous Bilayer Membranes on Charged Surfaces. Chem Lett. 1996:257–258.
32. Zhang L, Longo ML, Stroeve P. Mobile Phospholipid Bilayers Supported on a Polyion/Alkylthiol Layer Pair. Langmuir. 2000; 16:5093–5099.
33. Babiuk S, Baca-Estrada M, Babiuk LA, Ewen C, Foldvari M. Cutaneous Vaccination: the Skin as an Immunologically Active Tissue and the Challenge of Antigen Delivery. Journal of Controlled Release. 2000; 66:199–214. [PubMed: 10742580]
34. Glenn GM, Kenney RT, Ellingsworth LR, Frech SA, Hammond SA, Zoeteweij JP. Transcutaneous Immunization and Immunostimulant Strategies: Capitalizing on the Immunocompetence of the Skin. Expert Rev Vaccines. 2003; 2:253–267. [PubMed: 12899576]
35. Warger T, Schild H, Rechtsteiner G. Initiation of Adaptive Immune Responses by Transcutaneous Immunization. Immunol Lett. 2007; 109:13–20. [PubMed: 17320194]
36. Gill HS, Prausnitz MR. Coating formulations for microneedles. Pharm Res. 2007; 24:1369–1380. [PubMed: 17385011]
37. Boes M, Cerny J, Massol R, Op den Brouw M, Kirchhausen T, Chen J, Ploegh Hidde L. T-cell Engagement of Dendritic Cells Rapidly Rearranges MHC Class II Transport. Nature. 2002; 418:983–8. [PubMed: 12198548]
38. Zhang J, Chua LS, Lynn DM. Multilayered Thin Films that Sustain the Release of Functional DNA under Physiological Conditions. Langmuir. 2004; 20:8015–8021. [PubMed: 15350066]
39. Abramoff MD, Magelhaes PJ, Ram SJ. Image Processing with Image J. Biophotonics International. 2004; 11:36–42.
40. Prow TW, Chen X, Prow NA, Fernando GJP, Tan CSE, Raphael AP, Chang D, Ruutu MP, Jenkins DWK, Pyke A, et al. Nanopatch-Targeted Skin Vaccination against West Nile Virus and Chikungunya Virus in Mice. Small. 2010; 6:1776–1784. [PubMed: 20665754]

41. Ruutu MP, Chen X, Joshi O, Kendall MA, Frazer IH. Increasing mechanical stimulus induces migration of Langerhans cells and impairs the immune response to intracutaneously delivered antigen. Exp Dermatol. 2011; 20:534–536. [PubMed: 21457356]

42. Adams S, O'Neill DW, Nonaka D, Hardin E, Chiriboga L, Siu K, Cruz CM, Angiulli A, Angiulli F, Ritter E, et al. Immunization of Malignant Melanoma Patients with Full-Length NY-ESO-1 Protein Using TLR7 Agonist Imiquimod as Vaccine Adjuvant. J Immunol. 2008; 181:776–784. [PubMed: 18566444]

43. Mwangi W, Brown WC, Lewin HA, Howard CJ, Hope JC, Baszler TV, Caplazi P, Abbott J, Palmer GH. DNA-encoded fetal liver tyrosine kinase 3 ligand and granulocyte macrophage-colony-stimulating factor increase dendritic cell recruitment to the inoculation site and enhance antigen-specific CD4+ T cell responses induced by DNA vaccination of outbred animals. J Immunol. 2002; 169:3837–3846. [PubMed: 12244180]

44. Soiffer R, Lynch T, Mihm M, Jung K, Rhuda C, Schmollinger JC, Hodi FS, Liebster L, Lam P, Mentzer S, et al. Vaccination with irradiated autologous melanoma cells engineered to secrete human granulocyte-macrophage colony-stimulating factor generates potent antitumor immunity in patients with metastatic melanoma. Proc Natl Acad Sci U S A. 1998; 95:13141–13146. [PubMed: 9789055]

45. Akira S, Uematsu S, Takeuchi O. Pathogen Recognition and Innate Immunity. Cell. 2006; 124:783–801. [PubMed: 16497588]

46. Gay NJ, Gangloff M, Weber ANR. Toll-Like Receptors as Molecular Switches. Nat Rev Immunol. 2006; 6:693–698. [PubMed: 16917510]

47. Manicassamy S, Pulendran B. Modulation of Adaptive Immunity with Toll-Like Receptors. Semin Immunol. 2009; 21:185–193. [PubMed: 19502082]

48. Aucan C, Traore Y, Tall F, Nacro B, Traore-Leroux T, Fumoux F, Rihet P. High Immunoglobulin G2 (IgG2) and Low IgG4 Levels are Associated with Human Resistance to Plasmodium Falciparum Malaria. Infect Immun. 2000; 68:1252–1258. [PubMed: 10678934]

49. Beenhouwer DO, Yoo EM, Lai CW, Rocha MA, Morrison SL. Human Immunoglobulin G2 (IgG2) and IgG4, but Not IgG1 or IgG3, Protect Mice Against Cryptococcus Neoformans Infection. Infect Immun. 2007; 75:1424–1435. [PubMed: 17220317]

50. Nimmerjahn F, Ravetch JV. Divergent Immunoglobulin G Subclass Activity Through Selective Fc Receptor Binding. Science. 2005; 310:1510–1512. [PubMed: 16322460]

51. Krogman KC, Lowery JL, Zacharia NS, Rutledge GC, Hammond PT. Spraying asymmetry into functional membranes layer-by-layer. Nat Mater. 2009; 8:512–518. [PubMed: 19377464]

52. Kim YC, Quan FS, Yoo DG, Compans Richard W, Kang SM, Prausnitz Mark R. Enhanced Memory Responses to Seasonal H1N1 Influenza Vaccination of the Skin with the Use of Vaccine-Coated Microneedles. J Infect Dis. 2010; 201:190–198. [PubMed: 20017632]

53. Quan FS, Kim YC, Yoo DG, Compans RW, Prausnitz MR, Kang SM. Stabilization of Influenza Vaccine Enhances Protection by Microneedle Delivery in the Mouse Skin. PLoS One. 2009; 4:e7152. [PubMed: 19779615]

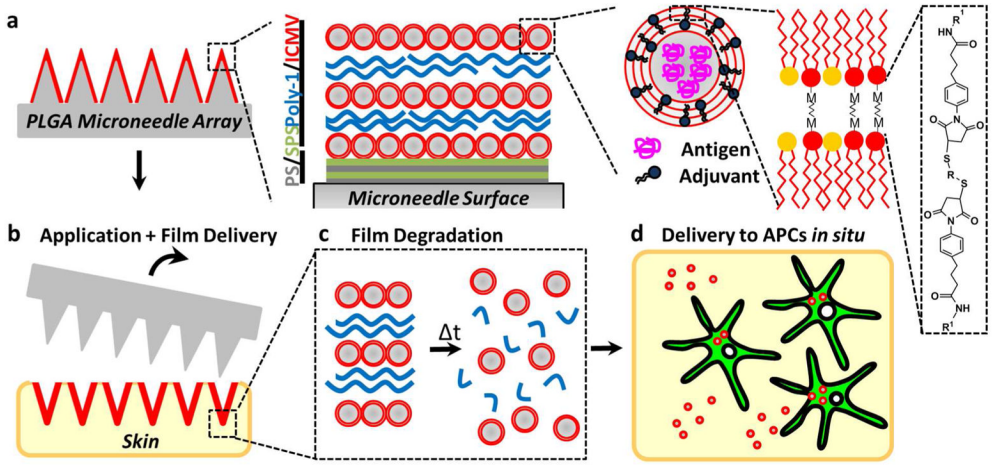


**Figure 1.**

(a) Schematic illustration of (Poly-1/ICMV) multilayers deposited onto PLGA microneedle surfaces. ICMV lipid nanocapsules are prepared with inter-bilayer covalent crosslinks between maleimide head groups (M) of adjacent phospholipid lamellae in the walls of multi-lamellar vesicles. (Poly-1/ICMV) PEMs were constructed on microneedles after (PS/SPS) base layer deposition. (b) Microneedles transfer (Poly-1/ICMV) coatings into the skin as cutaneous depots at microneedle insertion points. (c) Hydrolytic degradation of Poly-1 leads to PEM disintegration and ICMV release into the surrounding tissue. (d) ICMV delivery to skin-resident APCs provides coincident antigen exposure and immunostimulation, leading to initiation of adaptive immunity.

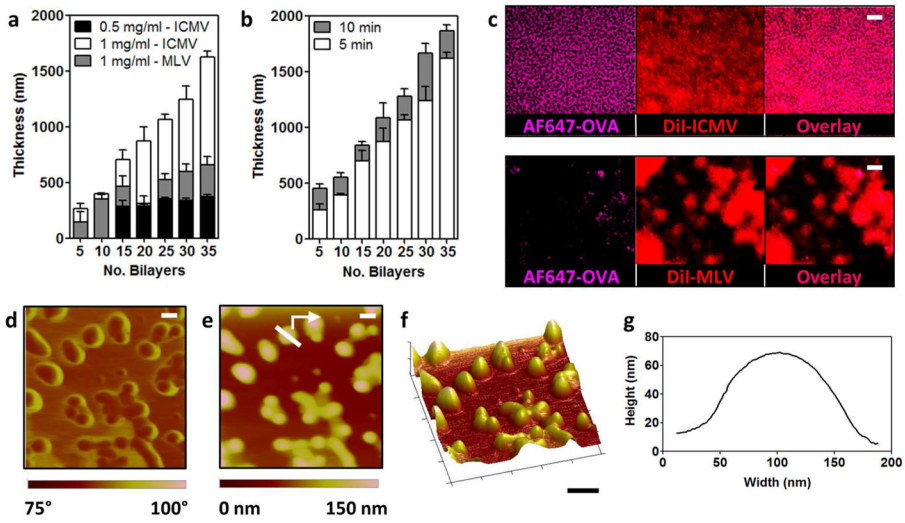


**Figure 2.**

Shown are poly-1/lipid film thicknesses determined by profilometry for deposited ICMVs or MLVs varying (a) concentration and (b) deposition time ($N = 12$). (c) CLSM image of $(PS/SPS)_{20}(Poly\text{-}1/ICMV)_{20}$ or $(PS/SPS)_{20}(Poly\text{-}1/MLV)_{20}$ multilayers deposited on silicon (scale bar ~ 20μm). ICMVs and MLVs contained AF647-OVA (pink) and were labeled with DiI (red). (d–g) AFM imaging of a dried $(Poly\text{-}1/ICMV)_5(PS/SPS)_{20}$ multilayers built on silicon (scale bar 100 nm). Shown are (d) phase, (e) height, and (f) 3-D rendered AFM height micrograph data for a $(Poly\text{-}1/ICMV)_5(PS/SPS)_{20}$ multilayer (scale bar 100 nm). (g) Height trace data (trace shown in panel (e) for a single embedded ICMV in a $(PS/SPS)_{20}(Poly\text{-}1/ICMV)_5$ multilayer.

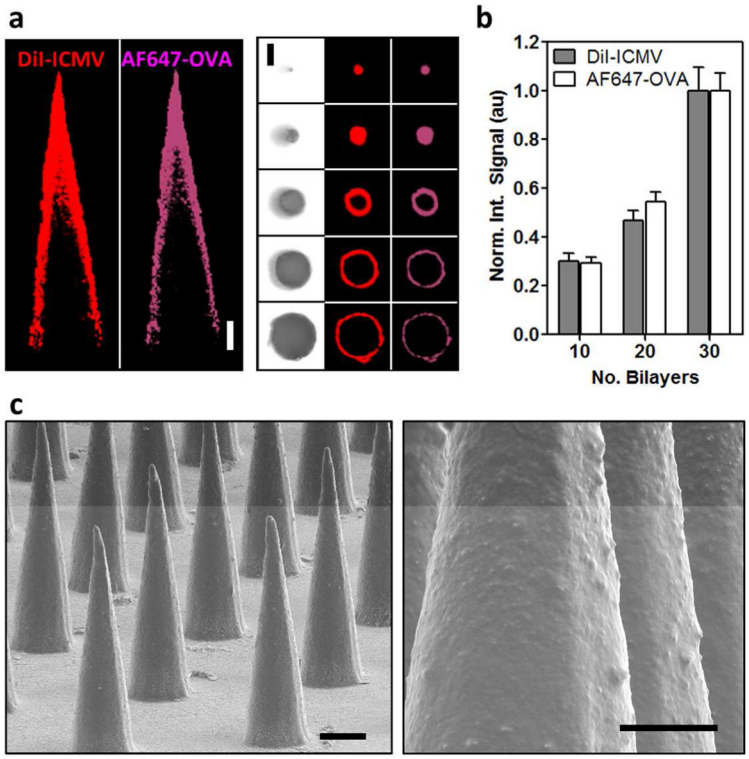


**Figure 3.**

(a) Representative confocal images of PLGA microneedles coated with $(PS/SPS)_{20}(Poly\text{-}1/ICMV)_{35}$ films (left, transverse optical sections; right, lateral sections; 100 μm interval; scale bar 100 μm; Red, DiI-ICMVs; Pink, AF647-OVA). (b) Quantification of DiI-ICMV and AF647-OVA incorporation into $(PS/SPS)_{20}(Poly\text{-}1/ICMV)_n$ films on microneedles. Analysis was performed using Image J measurement of total fluorescent signal intensity in confocal z-stacks collected along the length of microneedles, normalized to the total intensity obtained for 30 bilayer films (results shown are averaged from $N = 15$ individual microneedles per condition). (c) SEM micrographs of $(PS/SPS)_{20}(Poly\text{-}1/ICMV)_{35}$ multilayer-coated PLGA microneedles (scale bars: left 200 μm, right 50 μm).

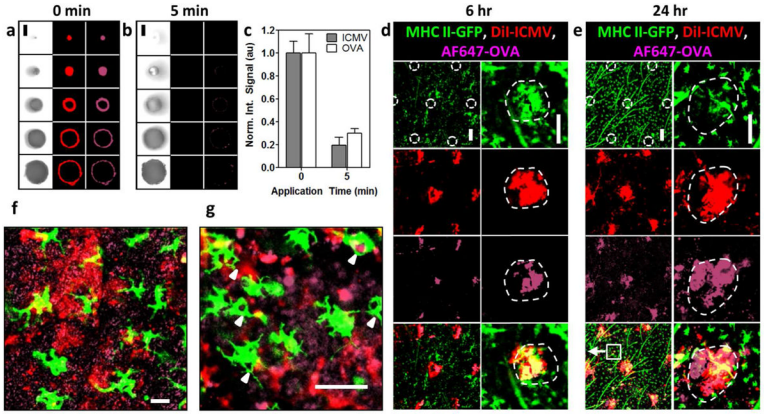


**Figure 4.**

(a–b) Representative confocal images of PLGA microneedles coated with $(PS/SPS)_{20}(Poly\text{-}1/ICMV)_{35}$ films before application (a) and after a 5 minute application to murine skin *IN VIVO* (b) (lateral sections, 100 μm *Z*-interval; scale bar 100 μm; Red, DiI-ICMVs; Pink, AF647-OVA). (c) Quantitation of confocal fluorescence intensities ($N = 15$) showing loss of DiI-ICMV and AF647-OVA films from coated microneedles upon application to skin. (d–g) Representative confocal images of mouse skin treated for 5 minutes with $(PS/SPS)_{20}(Poly\text{-}1/ICMV)_{35}$ multilayer-coated PLGA microneedles after (d) 6 hr or (e) 24 hr showing ICMV delivery at microneedle insertion sites (outlined). Shown is fluorescent signal from (top to bottom): MHC II-GFP (green), DiI-ICMVs (red), AF647-OVA (pink), and overlay (yellow) at low (left) and high (right) magnification (scale bars 100 μm). (f) High magnification CLSM image (field location highlighted by box in panel (e)) showing colocalization of ICMVs and OVA with APCs in the skin (scale bar - 20μm). (g) High magnification CLSM image showing APC phagocytosis of ICMVs with OVA after 24 hr (scale bar 20 μm).

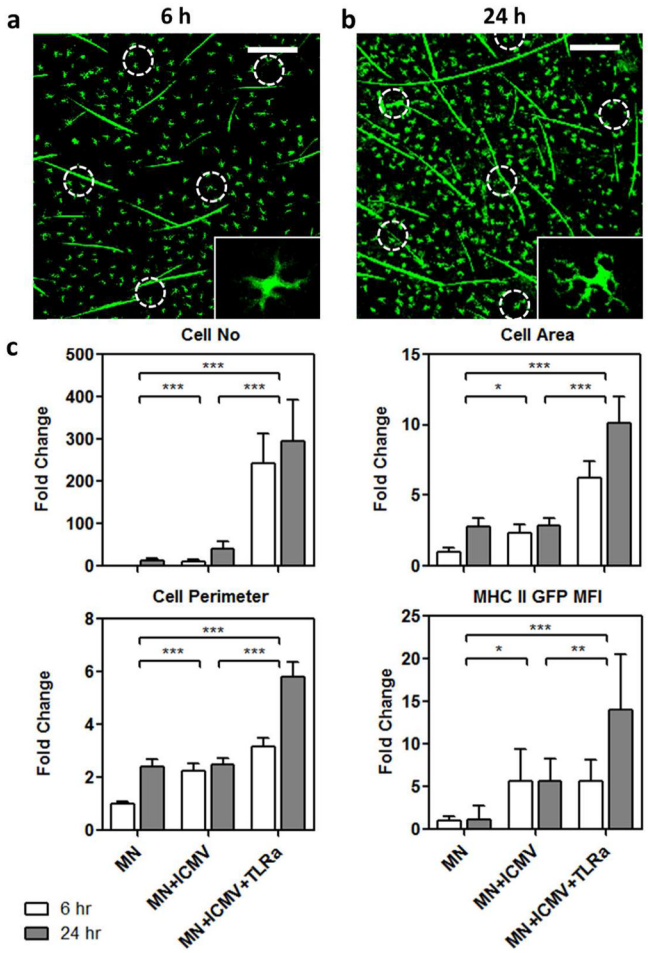


**Figure 5.**

Representative CLSM images of MHC II-GFP$^+$ cells in skin dissected (a) 6 or (b) 24 hours after $(PS/SPS)_{20}(Poly\text{-}1/ICMV)_{35}$–coated microneedle treatment for 5 minutes (insertion points outlined); ICMVs were loaded with MPLA and polyI:C was added to the skin directly before treatment (scale bar 200 μm). (c) Results of quantitative CLSM image analysis to determine total cell number per field, individual cell area and perimeter, and MHC II-GFP MFI, expressed as fold change relative to uncoated microneedle treated mice. Mice were either treated with uncoated microneedles (MN), or microneedles coated with $(PS/SPS)_{20}(Poly\text{-}1/ICMV)_{35}$ multilayers with or without added MPLA and polyI:C (MN+ICMV and MN+ICMV+TLRa, respectively). Data was analyzed for significance using two-way ANOVA (* - $p<0.05$, ** - $p<0.01$, *** - $p<0.001$).

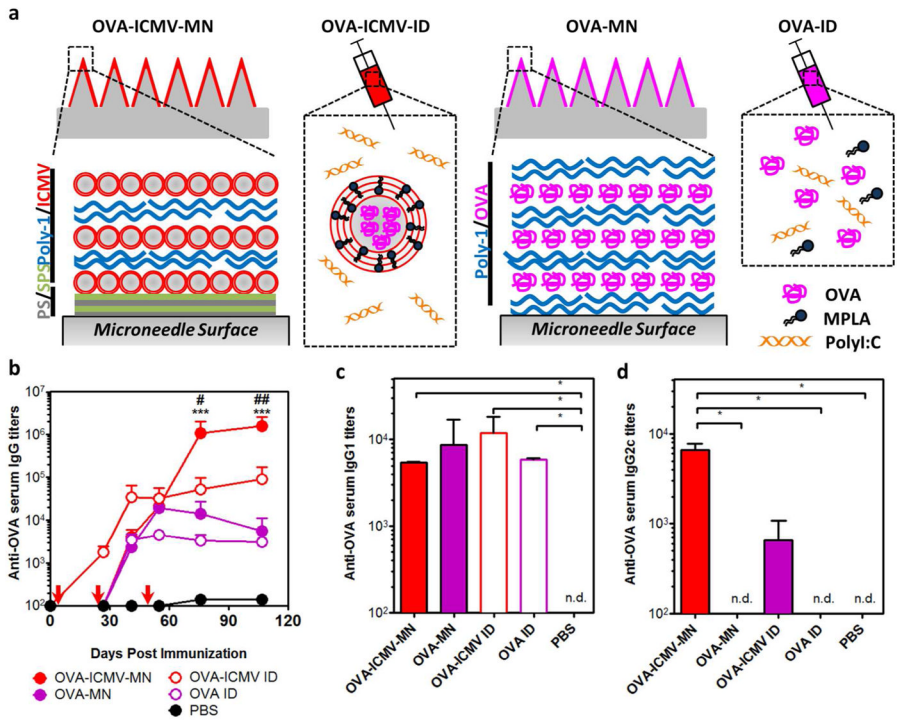


**Figure 6.**

(a) Schematic representation of vaccine treatments tested. (b) Anti-OVA serum IgG titers were measured over time with immunizations on days 0, 28, and 56 with OVA-ICMVs or soluble antigen administered *VIA* either microneedle-based multilayers or intradermal bolus injection at dorsal auricular skin. (c, d) Quantification of anti-OVA $IgG_1$ (b) and $IgG_{2c}$ (c) subtypes in sera at day 107. $^{\#}$, $P < 0.05$ and $^{\#\#}$, $P < 0.01$, compared to OVA-ICMV ID, and ***, $P < 0.001$, compared to OVA-MN or OVA ID, as analyzed by two-way ANOVA, followed by Tukey's HSD. *, $P < 0.05$, as analyzed by one-way ANOVA, followed by Tukey's HSD.